

Pore-Water Anomalies in Gas Hydrate-Bearing Sediments of the Deeper Continental Margins: Facts and Problems*

REINHARD HESSE

Department of Geological Sciences, McGill University, 3450 University St., Montreal, Quebec, H3A 2A7, Canada

(Received: 1 July 1988; in final form: 23 November 1988)

Abstract. Naturally occurring gas hydrates, discovered under the deeper parts of the continental margins (generally below 500 m water depth) during the Deep Sea Drilling Project and the Ocean Drilling Program, impregnate terrigenous sediments 0.5 to 1 km thick. They form from biogenic as well as thermogenic hydrocarbon gases and are associated with characteristic chemical and isotopic anomalies in the pore waters resulting from hydrate decomposition. Typical downward trends derived from water samples squeezed on board ship show decreasing chlorinity coupled with increases in the heavy oxygen and hydrogen isotopes resulting from the combined effects of sediment compaction and salt and isotope fractionation by hydrates. Carbon isotopes can be used to differentiate between biogenic ($\delta^{13}\text{C} < -55\text{\textperthousand}$) and thermogenic ($\delta^{13}\text{C} > -55\text{\textperthousand}$) gas hydrates except where acetate-derived methane is involved. Smooth downward trends in the chemical and isotopic anomalies suggest steady increases in the proportion of hydrates among the pore-filling substances. Spikes are attributed to high local hydrate concentrations (or massive hydrate layers or nodules). Problems encountered in delineating the detailed relationships between hydrate occurrence and pore-water anomalies concern (i) the roof-effect of a hydrate zone which should be marked by a positive Cl^- and a negative $\delta^{18}\text{O}$ anomaly (the opposite of the hydrate decomposition effect) (ii) the composition of *in-situ* pore waters from within hydrate zones; (iii) the suppression of a positive $\delta^{18}\text{O}$ hydrate-decomposition anomaly due to superposition of other oxygen-isotope fractionation effects (such as volcanic glass alteration); and (iv) the non-linear correlation between Cl^- depletion and ^{18}O enrichment, and the magnitude of the ^{18}O enrichment. The hydrate-decomposition mechanism still provides the most successful explanation for the chemical and isotopic porewater anomalies observed in hydrate-bearing sediments, but the problems encountered underscore the urgency for future research through deep-sea drilling in hydrate zones.

Key words. Gas hydrates; pore-water composition; chlorinity; oxygen, hydrogen, and carbon isotopes; hydrate-decomposition effect; roof effect; continental slope and rise.

1. Introduction

Clathrate hydrates are ice structures in which a framework of water molecules forms large voids that can accommodate guest molecules. In gas hydrates, the guest molecules are the gases such as CH_4 , CO_2 , H_2S , N_2 and many others, and these are not chemically bound in the structure but interact with it through van der Waals forces. Natural gas hydrates occur widespread under the permafrost zone in polar regions and in submarine hydrate-zones under the deep-sea floor in polar offshore areas (both in the Arctic and the Antarctic) but also in the tropical and subtropical

* Dedicated to Dr D. W. Davidson in honor of his great contributions to the sciences of inclusion phenomena.

oceans where sediments are particularly rich in organic matter. Hydrates are much more abundant on some other celestial bodies than on Earth, for example on Uranus, Neptune, Mars [1] and possibly on the Jupiter moons Europe, Ganimede, and Callisto.

Hydrate research has received major impetus from the discovery of gas hydrates under the sea-floor by the Deep Sea Drilling Project (DSDP) and the Ocean Drilling Program (ODP). The existence of submarine hydrate zones had first been postulated in 1966 by Sokolov [2] based on thermodynamic stability considerations and later by Stoll *et al.* (1971) based on evidence from seismic wave velocities [3]. Confirmation of these predictions by direct observation of gas hydrates in drill cores from the outer continental margins has been a major accomplishment of scientific deep-sea drilling. Hydrate-bearing sediments were first recovered in 1979 in drill-cores from the Middle America trench-slope off Mexico [4] and Guatemala [5]. These discoveries mark a turning point in the study of natural gas hydrates extending their known occurrence from permafrost regions on land to wide areas beneath the sea on continental slopes and rises. The first observation of hydrate-bearing sediments from a subaqueous environment was actually reported from an inland sea, the Black Sea [6]. The association with the outer continental margins of the major oceans, however, is more typical for submarine hydrate zones, because temperature and pressure conditions under the deep-sea floor are suitable for hydrate stability, and high organic-matter content of the sediment causes methane generation in amounts sufficient for hydrate formation. The ocean basin floors, which are also within the hydrate stability field, in contrast, are devoid of hydrates because of inadequate preservation of reactive organic matter from which methane can be generated. The sites of the first discoveries of submarine hydrate-zones (Pacific continental margin of Central America [4, 5]; Blake-Bahama Outer Ridge off the East Coast of the United States [7], together with those of subsequent discoveries, for example on the South American active margin off Peru [8]), have now become well-studied, classical deep-water hydrate localities. Much of the information on the chemistry of hydrate-related pore waters discussed in this paper comes from these three localities.

2. Chemical Trends in Pore-Water Composition of Deep-Marine Sediments

Since the first recovery of gas hydrates in drill-cores from the Middle America trench slope, it was noticed that pore-waters squeezed from hydrate-bearing sediments show two specific anomalies in their chemical and isotopic composition [9], namely a downhole chloride decrease coupled with a $\delta^{18}\text{O}$ increase. These anomalies have recurrently been observed at most hydrate sites. In order to demonstrate that they are uniquely associated with hydrate-bearing sediments, the chemical trends in the pore-water composition of deep-marine sediments established by scientific deep-sea drilling will be reviewed in the first part of this paper. This discussion will show in particular that any evidence for unspecified alternative mechanisms postulated by Finley and Krason (1986) for the coupled chloride-oxygen isotope anomalies [10, 11] is lacking. The observed anomalies can therefore be used to predict the presence of gas hydrates, if no other evidence is available. They cannot yet be used to quantitatively estimate hydrate abundance. In the

second part of the paper, an evaluation of the details of these hydrate-related pore-water anomalies will be presented.

As a result of the interstitial water sampling program of the DSDP and its successor program, the ODP, pore-water analyses are now available from virtually every sedimentary environment under the modern ocean basins and continental margins. Progress in data collection and interpretation has been summarized during various phases of the drilling programs [12–18]; and chemical trends have now been firmly established for most offshore areas to at least 400 to 500 m subsurface depth, and for many areas to much greater depths. For the hydrate problem, the upper 500 m of the sediment column are of greatest interest because in many areas, hydrates decompose at greater subsurface depth. Based on several hundred drill-holes for which pore-water analyses are available, a broad classification of pore-water profiles into three groups with a total of nine different types may be proposed (Figure 1). These are end-member types which embrace the major variations in pore-water chemistry that occur in modern offshore sedimentary basins and physiographic provinces of the ocean floors. In this paper, the different types will be briefly discussed highlighting their salient features in order to compare them with the characteristics of hydrate-related pore waters. A more detailed discussion is to be found in [18].

2.1. PORE-WATER CHEMISTRY IN OXIC TO SUBOXIC PELAGIC AND HEMIPELAGIC SEDIMENTS OF THE OPEN OCEANS (LOW TO INTERMEDIATE SEDIMENTATION-RATE BASINS; PROFILE TYPES 1 TO 3).

Pore-water in pelagic and slowly deposited hemipelagic sediments of the open oceans are either straight or only moderately curved vertical lines. The straight-line profiles (type 1, Figure 1) with sea water composition all the way down to the basaltic basement of the oceanic crust obviously are the simplest possible type of profiles. Such simple trends are very unusual, however, and are not what one would expect to find, in view of diagenetic reactions and diffusion taking place in oceanic sediments. According to McDuff (1981), this simple chemistry may represent convection-controlled profiles on young oceanic crust characteristic of intake (recharge) areas for sea water [17]. Deeper in the crust, the water is heated up and entrained in hydrothermal convection cells. The discharge areas at the other end of these cells are the hydrothermal vent systems best known from the 'black and white smokers' on the crest of mid-ocean ridges. The ridge crest is not the only discharge region for hydrothermal fluids, because the ridge flanks are underlain by a series of convection cells [19–21]. Although convection seems to be fast enough in the intake areas to wipe out any chemical gradients that might result from reactions in the sediment, it does not seem to be capable of suppressing geothermal gradients entirely (see [22] for further references).

Slightly curved pore-water profiles are found in pelagic or hemipelagic sediments with minor early diagenetic reactions as indicated by the slight sulfate decrease in type 3. This decrease results from bacterial sulfate reduction which is coupled with organic-matter oxidation. More strongly curved profiles are observed in diffusion-dominated sections of the pelagic realm (type 2, Figure 1). In the latter, calcium and magnesium are typically negatively correlated with Ca increasing and Mg

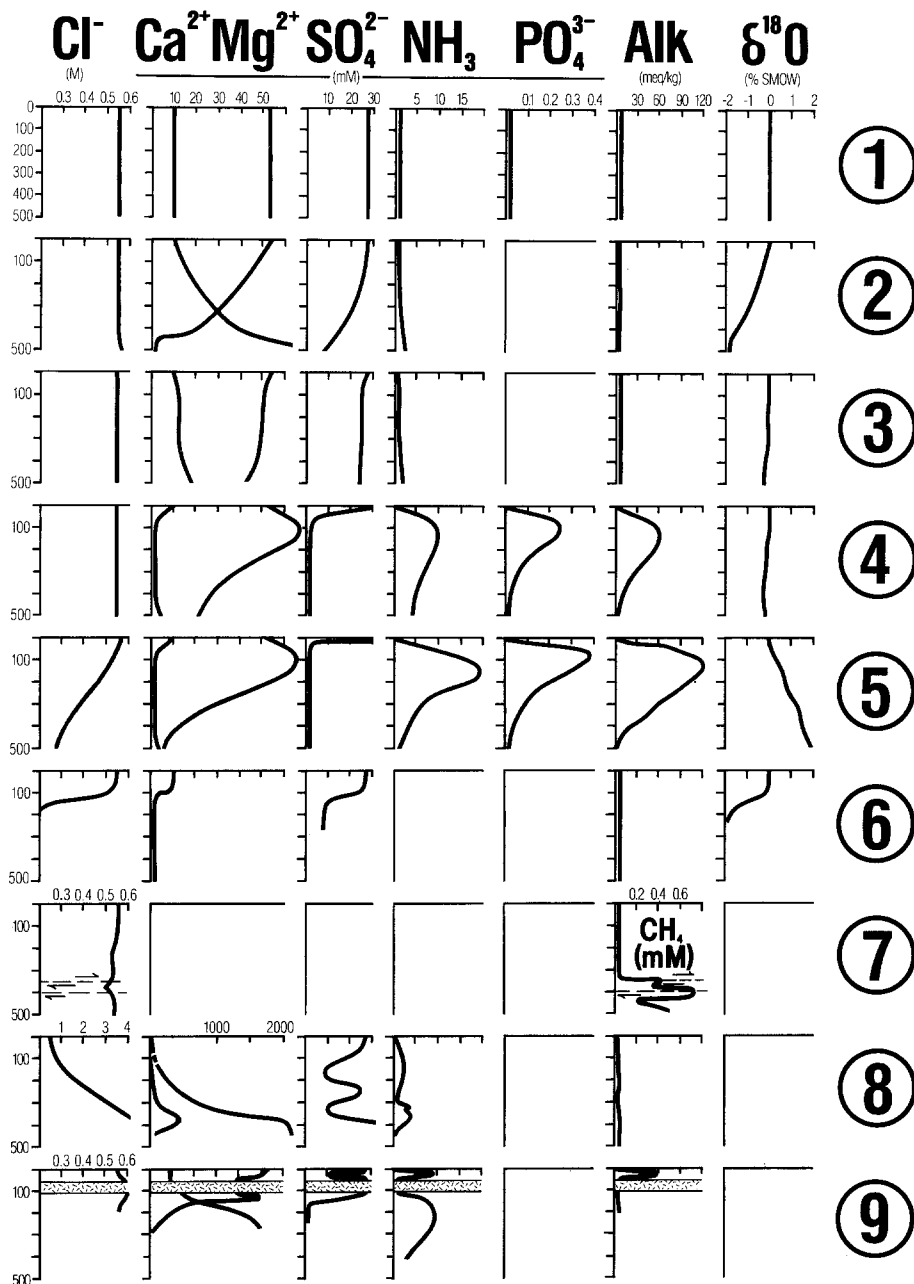


Fig. 1. Major types of interstitial water profiles: 1–3: Oxic and suboxic pelagic and hemipelagic sediments (low to intermediate sedimentation rate basins); 1: convection-controlled; 2: diffusion-controlled with linear correlation between changes in Ca and Mg concentration; 3: reaction-controlled suboxic environments; 4, 5: reaction-controlled anoxic terrigenous and hemipelagic sediments of the continental margins without (4) and (5) with gas hydrates; 6: fresh-water influx in an aquifer at depth; 7: lateral pore-water advection along fault zones; 8: evaporite dissolution at depth in the subsurface; 9: hydrothermal activity and intrusion of igneous sills and dikes.

decreasing downwards [23]. The oceanic crust is a sink for Mg which is taken up by alteration reactions in the basalt involving the formation of secondary minerals such as brucite or saponite. It is a source for Ca which is released by hydrolysis reactions from silicates. Convex downward curvature of the profiles illustrates downward decreasing diffusion coefficients as both compaction and cementation of the sediments increase with burial depth [24]. A convincing argument in favor of diffusion as the dominant factor controlling the shape of these profiles is the linear correlation between the Ca change (negative correlation) or the Mg change (positive correlation) and oxygen isotope variation. $\delta^{18}\text{O}$ values become increasingly more negative downwards as basement is approached. The only significant fractionation mechanism in pelagic sediments that can produce such a negative $\delta^{18}\text{O}$ shift is the removal of heavy oxygen from the pore water by the formation of clay minerals and zeolites from volcanic glass or basaltic minerals [25, 26]. This shift is of particular interest with respect to hydrate-related pore waters which show the opposite trend as discussed below. In these diffusion-dominated profiles, the minimum in the $\delta^{18}\text{O}$ curve will occur at the base of the drill hole, if volcanic-matter alteration occurs in the basalt of the oceanic crust. It may occur in mid-section, if ash layers are involved that are interstratified with the pelagic or hemipelagic sediment (see site 565 below).

The host sediments for type 1 to 3 pore-water profiles mostly remain oxidized throughout their burial history or may become suboxic in cases where some reactive organic matter is retained by the sediment. In the latter case, nitrate reduction occurs in the pore water after exhaustion of the dissolved oxygen. The process may even lead to the initiation of sulfate reduction as schematically indicated by the type-3 profile (Figure 1). The more pronounced sulfate decrease in type 2, by contrast, is caused by diffusion of sulfate into the oceanic crust.

2.2. REACTION-CONTROLLED PORE-WATER PROFILES IN ANOXIC TERRIGENOUS AND HEMIPELAGIC SEDIMENTS OF THE CONTINENTAL MARGINS (HIGH SEDIMENTATION-RATE BASINS; PROFILE TYPES 4 AND 5).

Pore-water profiles in gas hydrate bearing sediments belong to the second family of profiles characteristic for high sedimentation-rate areas on the continental margins (with rates of at least 100 m/Ma, but often in excess of 500 m/Ma). The hydrate-related profiles (type 5) are a modification of the normal high sedimentation-rate profiles (type 4) with which they share their principal characteristics. They are distinctly different from the first group of profiles discussed in the previous section in that they display strong concentration gradients, particularly in the upper parts of the sampled sedimentary section. These gradients are indicative of vigorous early diagenetic reactions. Compared to the low accumulation-rate pelagic sediments (with sedimentation rates generally less than 50 m/Ma and often less than 5 m/Ma), the rapidly deposited continental margin sediments retain much of the organic matter that is supplied to the sea floor along with the detrital and biogenic sediment constituents. The consequence of rapid deposition and short residence time on the sea floor is a high preservation factor for organic matter. The organic matter which is of marine or terrestrial origin will be buried before it is exposed for long periods of time to oxidizing bottom waters on the sea floor. In these sediments, organic

carbon (C_{org}) generally exceeds 1% wt; at some recently drilled gas hydrate sites on the Peruvian active margin (i.e. sites 682 and 688, ODP leg 112, [8]) C_{org} concentrations in excess of 8% were encountered.

Organic-matter rich sediments are diagenetically very reactive from the first moment of burial. The organic matter is subject to extensive microbial attack. The organic decomposition products in turn trigger inorganic mineralization reactions such as iron sulfide and carbonate precipitation. Bacterial organic matter oxidation involves different reservoirs of oxidants which are depleted in a characteristic sequence, one after the other. This sequence which is determined by decreasing free-energy changes associated with each of the various oxidation reactions [27] consists of (1) freely dissolved oxygen ('oxidation zone'), (2) nitrate, (3) sulfate, (4) carbonate (methane generation zone), and (5) the organic matter itself (fermentation zone) (Figure 2). (6) At temperatures above 60–70°C, activation energies for spontaneous organic-matter breakdown are reached. Thermocatalytic reactions include, among others, the decarboxylation of organic acids. Typical decomposition products released by these oxidation reactions are ammonia, phosphate and bicarbonate/carbonate. Their release is reflected by the steep maxima for these nutrients

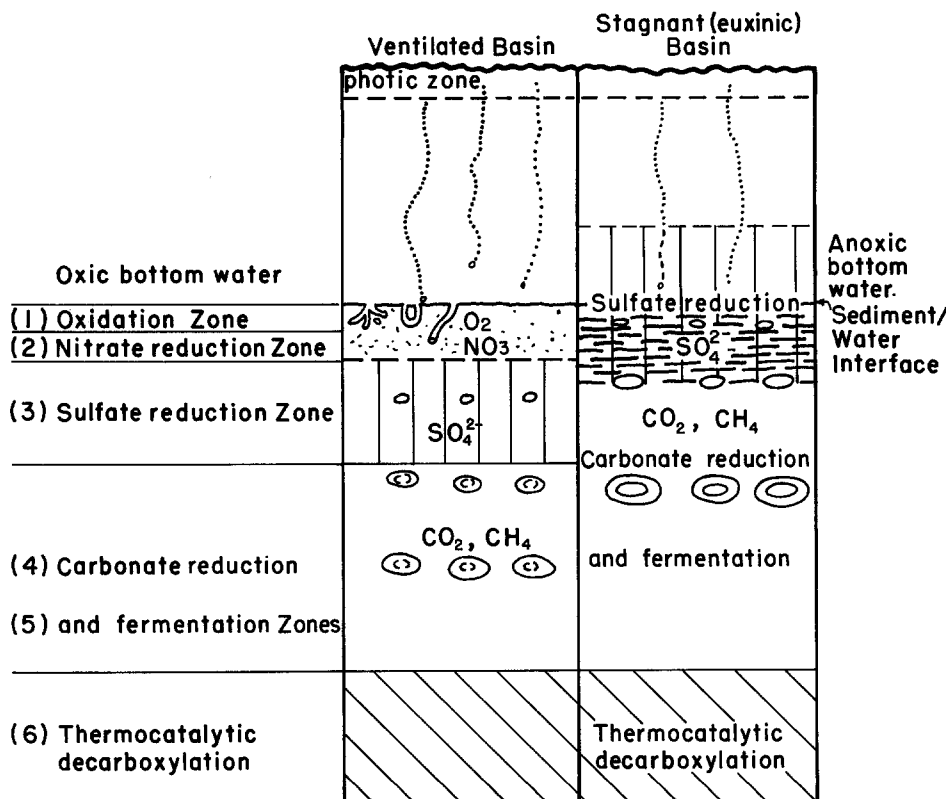


Fig. 2. Stages of organic-matter oxidation in anoxic sediments. Ellipses indicate concretion growth. (Modified from [28]).

and alkalinity in the upper 100 to 200 m of the sedimentary section (type-4 profiles). Sulfate depletion in organic-matter rich sediments rapidly leads to exhaustion within the upper few meters to few tens of meters. Free oxygen may disappear a few centimeters or tens of centimeters from the sea floor. Below, the sediment is anoxic.

Immediately below the sulfate-reduction zone, microbial methane generation commences which produces the methane for hydrate formation. Methane forms from carbonate reduction as shown by the parallelism in the carbon-isotopic composition between these two carbon-bearing species (Figure 3). The bacterially produced methane has $\delta^{13}\text{C}$ values about 70‰ lighter than those of the CO_2 from which it forms. As the residual CO_2 gets progressively heavier in the course of this Raleigh distillation process, so also does the methane. In the methane-generation zone, CO_2 is initially produced at a faster rate than it is consumed by bacterial reduction as shown by the alkalinity maximum which occurs *within* the carbonate-reduction/methane-generation zone rather than at its top (Figure 4). The precipitation of solid carbonates also contributes to the alkalinity decrease with depth. The overall effect of organic-matter oxidation in the methane zone which involves a complex series of fermentation reactions can be described as a disproportionation reaction producing CH_4 and CO_2 simultaneously.

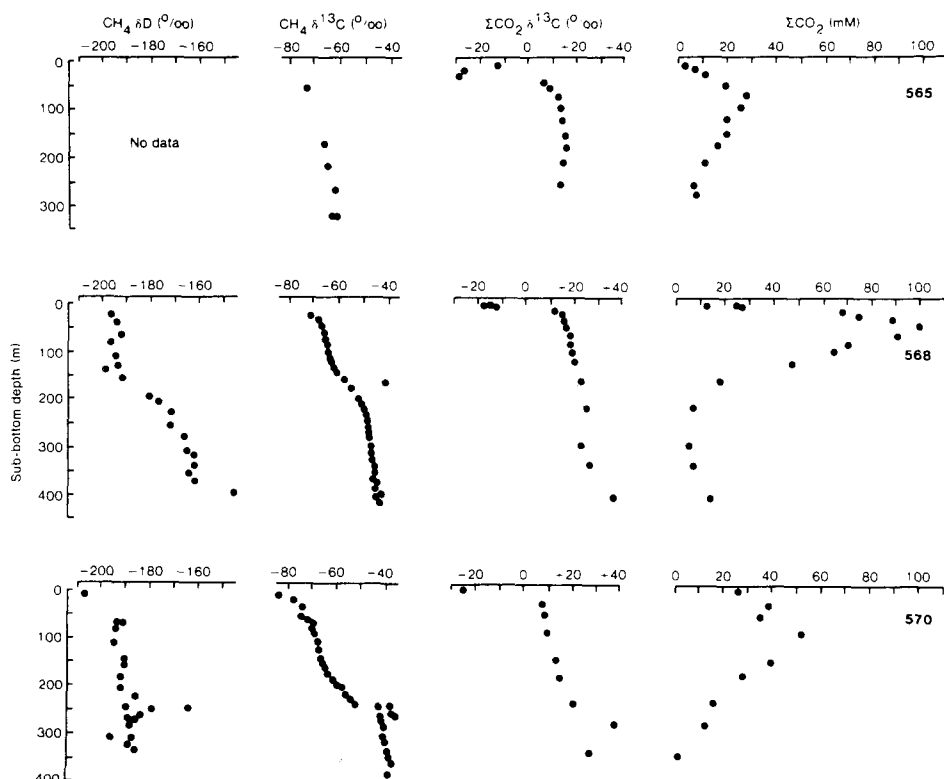


Fig. 3. Hydrogen and carbon-isotope composition of methane and carbon dioxide in drill sites 565, 568, and 570 on Middle America trench slope off Costa Rica (565) and Guatemala (568, 570) [29].

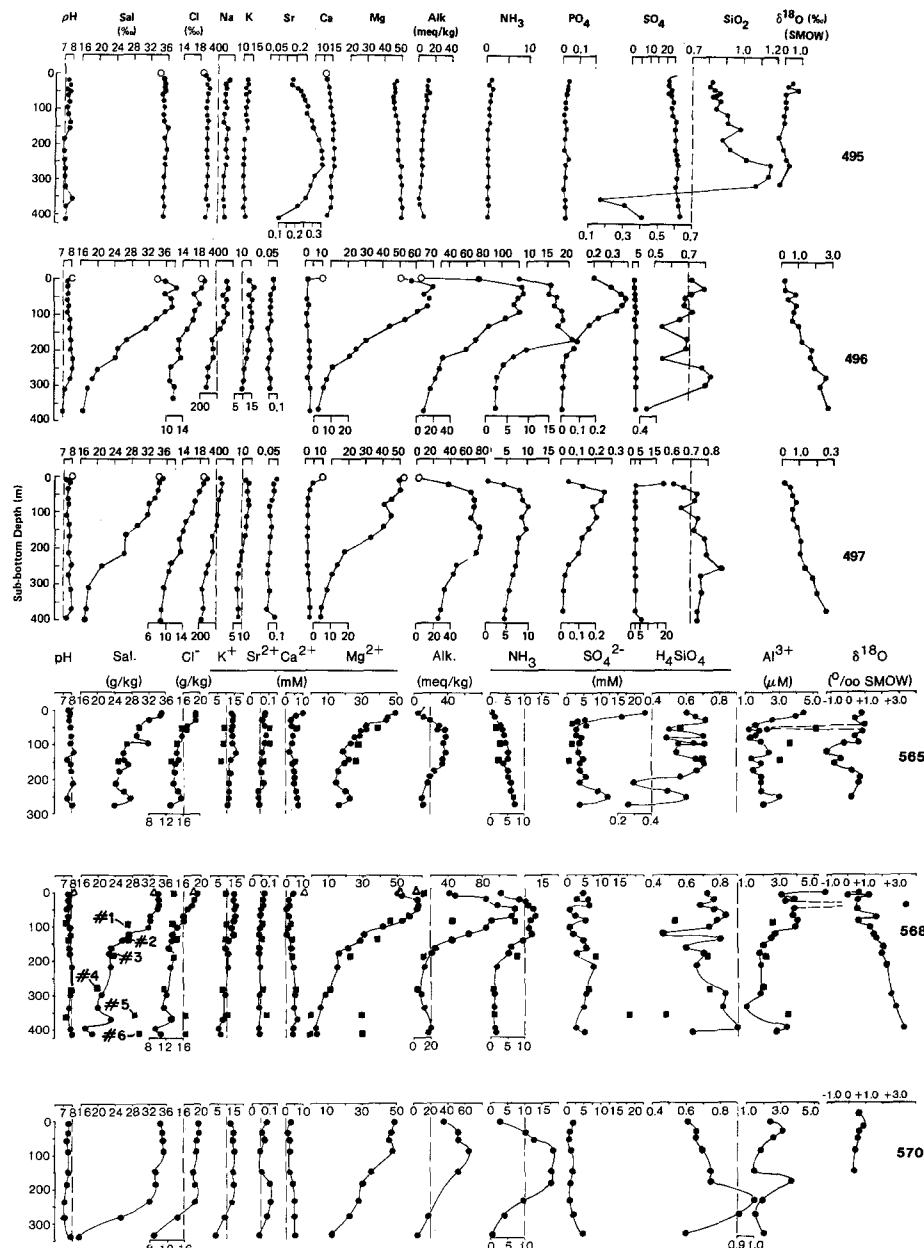


Fig. 4. Pore-water chemistry and oxygen-isotopic composition of DSDP drill sites 495 (mixed type 1–2–3 pore-water profile), 496 (type 5), 497 (type 5), 565 (type 5), 568 (type 5), 570 (type 5) on Middle America trench slope and adjacent oceanic crust (site 495) [30, 31]. Numbered squares: *In-situ* water samples.

The maxima for NH_3 and PO_4^{3-} occur at the same depth as the alkalinity maximum or somewhat deeper (Figure 4). The removal processes for PO_4^{3-} involve precipitation of collophane and apatite, and probably also adsorption. There are no known stable ammonia-bearing minerals in anoxic deep-sea sediments. Ammonia removal probably occurs largely by ion-exchange reactions with clays. In oxic pelagic sediments, ammonium ions are incorporated into inter-layer positions of clay minerals with high layer charges, particularly vermiculites and illites [32]. Similar fixation mechanisms probably exist in anoxic, organic-matter rich sediments. Note that despite the strong vertical variations shown in Figure 1, type-4 profiles display constant chloride concentration and oxygen isotope ratio because these species are not involved in reactions in normal high-sedimentation rate sections.

Hydrate-bearing sections (type 5) show essentially the same characteristics as the high-sedimentation rate profiles of type 4 with the specific hydrate anomalies for chlorinity and $\delta^{18}\text{O}$ added (Figure 1). The gradients of type-5 profiles are even higher with more accentuated maxima than those of type-4 profiles for hydrate-free sediments of similar chemical and mineralogical composition.

Gas hydrate formation is due to rapid bacterial methane generation which in these organic-matter rich sediments takes place at very shallow subsurface depth after the completion of sulfate reduction. The methane may also be thermally generated at greater subsurface depth and move up along fault-zones as indicated for the pore-water profiles of type 7. So far, evidence for lateral pore-fluid advection in the sediment column has only been encountered in the imbricated sediment wedge under the active-margin slope off the Lesser Antilles (ODP drill sites 671 and 674 off Barbados [33]) on which the schematic profile type 7 (Figure 1) is based. Thermogenic gas hydrates have been recovered from several localities in the Gulf of Mexico [34–36] and also the northern California continental slopes [37] where the occurrence of hydrates had been predicted by Field and Kvenvolden (1986) [38]. Thermogenic or mixed biogenic/thermogenic hydrates are characterized by (i) a relatively heavy carbon-isotopic composition of the methane and (ii) relatively large proportions of ethane, propane, isobutane and even *n*-butane. The presence of *n*-alkanes larger than C_2 suggests the occurrence of structure-II hydrates besides structure-I hydrates, because only the former contain cages of proper size in their crystal lattices to accept these higher hydrocarbons. Thermogenic hydrates appear to be composed of predominantly structure-II hydrates and biogenic hydrates of predominantly structure-I [35]. Methane $\delta^{13}\text{C}$ values determined for thermogenic hydrates range from -41 to $-56\text{\textperthousand}$ [34, 35], whereas biogenic methane is generally lighter than $-55\text{\textperthousand}$ [39] except where it is derived from an acetate substrate [40]. Thermogenic hydrates have been found in piston cores as close as 1 m below the sea floor [35].

2.3. PORE-WATER ANOMALIES IN SPECIAL ENVIRONMENTS (PROFILE TYPES 6, 8, 9).

Before addressing the hydrate-specific pore-water anomalies, some other pore-water anomalies encountered in a variety of environments will be dealt with. The purpose of this enumeration is to further demonstrate that no other environment associated with pore-water anomalies produces the combination of decreasing chlorinity and increasing $\delta^{18}\text{O}$ values with depth observed in hydrate zones.

For example, in profile type 6 (Figure 1), the chemical and isotopic effects of fresh-water influx in aquifers at depth are depicted. Such profiles also display a downward chlorinity decrease which may be much more abrupt than that observed in hydrate zones depending on how recently the flow system has been active. In contrast to hydrate zones, however, meteoric-water influx is accompanied by a negative rather than a positive $\delta^{18}\text{O}$ anomaly.

Increases in the heavy oxygen isotope of interstitial waters with depth have been inferred [41] or observed [42] on a regional scale in sedimentary basins. They are due to isotopic exchange reactions between the fluids and the solids at more elevated temperatures above 50°C. Although the $\delta^{18}\text{O}$ increase is principally similar to that seen in hydrate zones, it is (i) not systematically associated with a chlorinity decrease and (ii) occurs at significantly greater burial depths than the thermodynamic stability field of gas-hydrates.

Whereas profile types 5 (hydrate zone) and 6 (fresh water influx) display significant downward chlorinity decreases, evaporite dissolution at depth produces a downward chlorinity increase that may be very pronounced (profile type 8, Figure 1; notice difference in scale between this profile which is in moles and the other chloride profiles which are in decimoles). Slight chlorinity increases in the vicinity of igneous dikes and sills may result from hydration reactions associated with the intrusion of such bodies (type 9, Figure 1).

The depth trends in pore-water composition illustrated in Figure 1 are all schematic. However, they are based on information from thousands of water analyses and summarize the information available from more than 70 cruises of the DSDP and ODP. Although no claim of completeness is intended with the diagrams of Figure 1, it is probably safe to assume that they cover the major environments and processes affecting the chemical composition of interstitial waters in deep-sea sediments. It may be concluded therefore that pore-water anomalies similar to those associated with hydrate zones do not occur elsewhere in hydrate-free sediments residing within the thermodynamic stability field for hydrates at shallow to intermediate burial depths. On the other hand, as shall be pointed out later, hydrate-bearing sediments are not 100% associated with the typical hydrate pore-water signature.

3. Salt and Isotope Fractionation Associated with Gas-Hydrate Formation

When a downhole chlorinity decrease in the pore waters of hydrate-bearing sediments was first detected during deep-sea drilling on the Middle America trench slope off Guatemala (DSDP drill sites 496, 497, Leg 67 [30]), it was initially interpreted as evidence for fresh-water influx similar to that seen under the Florida continental shelf. There, fresh water penetrated Tertiary limestone aquifers during the Pleistocene low sea-level stands to considerable subsurface depth and distances up to 120 km from shore causing complete freshening of the pore fluids below an upper salt-water lid. However, considering the complex geology of the Middle America trench slope and the great water depth of the drill holes in which the chlorinity anomaly was observed, the fresh water reflux model became a rather remote and unlikely possibility, particularly in view of the fact that gas-hydrates might provide an alternative explanation for the anomaly. The range of subsurface

depths (up to 5 km and more) and distances from land (up to 100 km) involved would be too great to recirculate non-saline ground waters through deep aquifers back into the ocean without altering them to saline deep-basin brines. In addition, the geologic structure of the margin with its listric normal faults at shallow subsurface depths and its imbricated stack of thrust sheets and tectonic slivers at greater depth would seem to present an impenetrable barrier to fluid flow (Figure 5), particularly for a drill site like 498 in one of the deeper, imbricated tectonic slices.

The possibility that gas-hydrates may provide an explanation for the subsurface freshening of the pore waters arose from the property of hydrates not to incorporate sea salts in their crystal structures, like normal ice. Hydrate formation would thus cause salt fractionation. As fresh water is withdrawn from the pore-water reservoir in the course of hydrate crystallization, the remaining interstitial water would become progressively more saline, provided the methane generation process required for hydrate formation is not associated with large-scale water production. This salt fractionation combined with the expulsion of pore-water from the sediment as it subsides during burial would explain the downward freshening trend of the pore water. At first glance, this interpretation may sound contradictory because the portion of the pore water not involved in hydrate formation becomes progressively more saline as more hydrate forms. The freshening, however, is an artifact of the sampling procedure which involves hydrate decomposition in the course of sample retrieval.

Compaction, in a very simplistic way, may be viewed as the solids sinking through a pore-water column of increasingly smaller cross-section as in the funnel model of Figure 6a. The solids subside, but the fluids basically stay where they are. This model, of course, is a gross oversimplification, but it illustrates the basic principle of the compaction mechanism. Natural sediments obviously do not compact by lateral contraction. To make the model geologically more realistic, the funnel will have to be turned 90° as in Figure 6b. The various slices representing layers of progressively compacted bulk sediment will also have to be separated and stacked in a vertical sequence as in Figure 6c. The gas hydrate crystals form part of the solid fraction of the sediment and subside with the other solid materials. As long as sufficient porosity remains to retain some permeability, pore fluids from a given subsiding sediment layer can be expelled upwards into the next overlying layer as the sediment subsides deeper, thus causing partial separation of the solid grains from their original pore-fluids. When the hydrates have subsided to the base of the hydrate zone and decomposed, the hydrate water, which is fresh water, will remix with a substantially reduced pore-water volume. Although this pore-water should be saltier than the original sea water, its reduced volume should result in a substantial freshening upon remixing with the hydrate water. The same conditions apply to the decomposition of hydrates when hydrate-impregnated sediment is brought up from the low temperatures and relatively high pressures (of several 100 bars) under the deep-sea floor. Here the freshening of the pore water becomes an artifact of the sampling process.

The hydrate mechanism of pore-water freshening can be tested by another hydrate-related fractionation which affects isotopes. Hydrates concentrate heavy isotopes in their structure upon crystallisation from the pore fluid. This isotopic

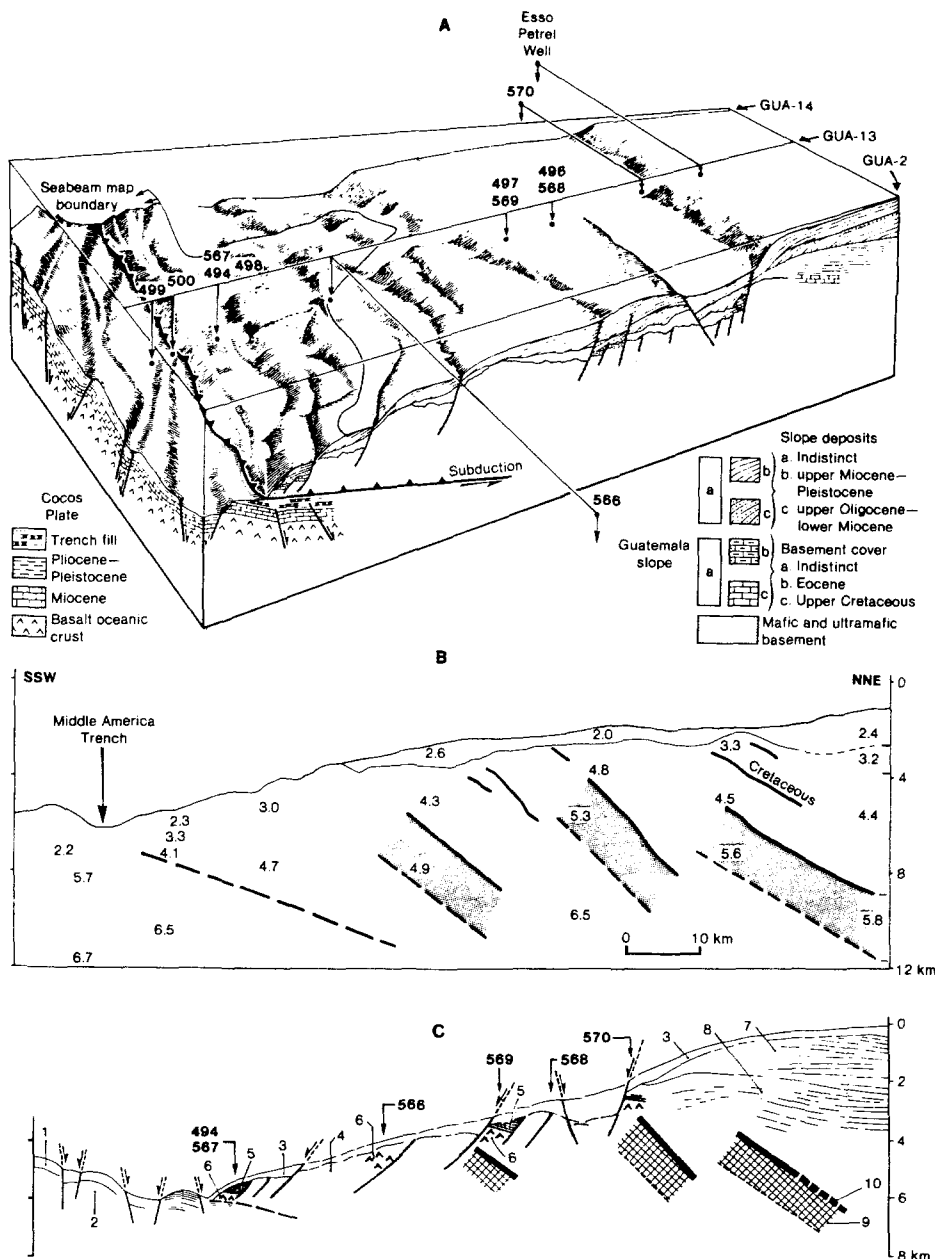


Fig. 5. Convergent extensional margin of the Middle America trench slope off Guatemala and location of drill sites of DSDP Legs 67 and 84 (from [43]). A: Listric normal faults at shallow subsurface depth. B: Summary of velocity structure and major landward dipping reflectors in pre-Campanian ophiolite slabs (based on seismic reflection and refraction studies). C: Geologic interpretation of Guatemalan margin structure. Miocene to Quaternary pelagic and hemipelagic sediments (1) and basalt (2) of subducting Cocos plate; Plio-Pleistocene slope apron of hemipelagic and terrigenous sediments (3); acoustic basement (4); Upper Campanian to Miocene sediments (5) and peridotites (6) of imbricated thrust sheets; Oligocene-Miocene (7) and Paleocene-Eocene (8) forearc sediments; Upper-Jurassic to Upper Cretaceous ophiolite (9) and major seismic reflector (10).

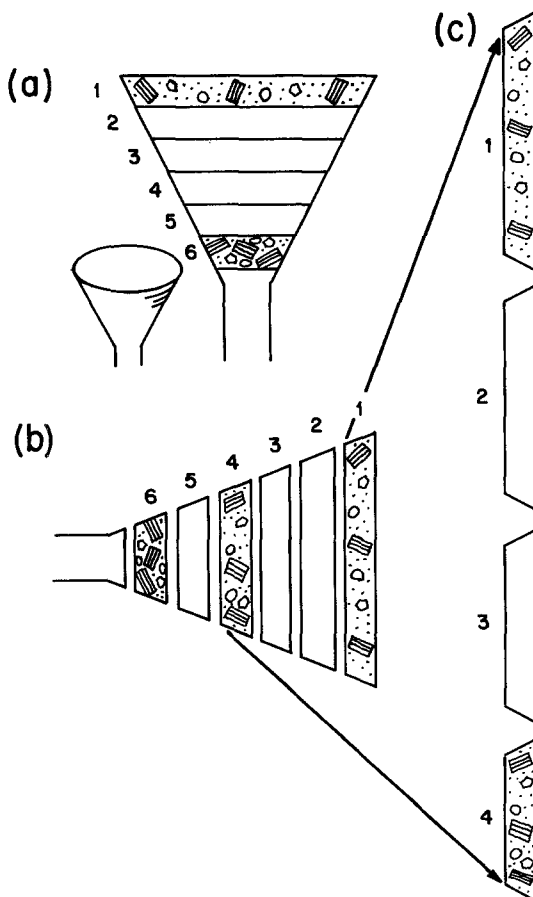


Fig. 6. Funnel model of compaction and sediment dewatering (see text for explanation). Pentagonal rings = hydrate crystals, book-shaped rectangles = clay minerals, dots = pore water.

fractionation together with the compaction mechanism just described leads to enrichment of the pore-waters in the heavy isotopes upon hydrate dissociation in the same way as outlined for the water-freshening mechanism.

The two processes – salt fractionation and isotope fractionation combined with the effects of compaction – thus explain qualitatively the observed pore-water anomalies in hydrate zones: a downward decrease in chlorinity and an increase in the $\delta^{18}\text{O}$ values. The same holds for δD values.

Smooth $\delta^{18}\text{O}$ and chlorinity versus depth profiles as displayed, for example, by DSDP sites 496, 497, and 568 (Figure 4) suggest steady increases with depth in the portion of the bulk volume taken up by hydrates or may be produced by diffusion as suggested for the upper part of site 570 (Figure 7). In fine-grained sediments, the hydrate crystals are probably finely disseminated. Normally, they cannot be observed because they appear to decompose before the sediment cores are split and inspected on board ship.

Large fluctuations in ^{18}O and chloride with depth as, for example, observed in DSDP Leg 66 sites [44], at DSDP site 533 (Leg 76, Figure 8), and locally at some

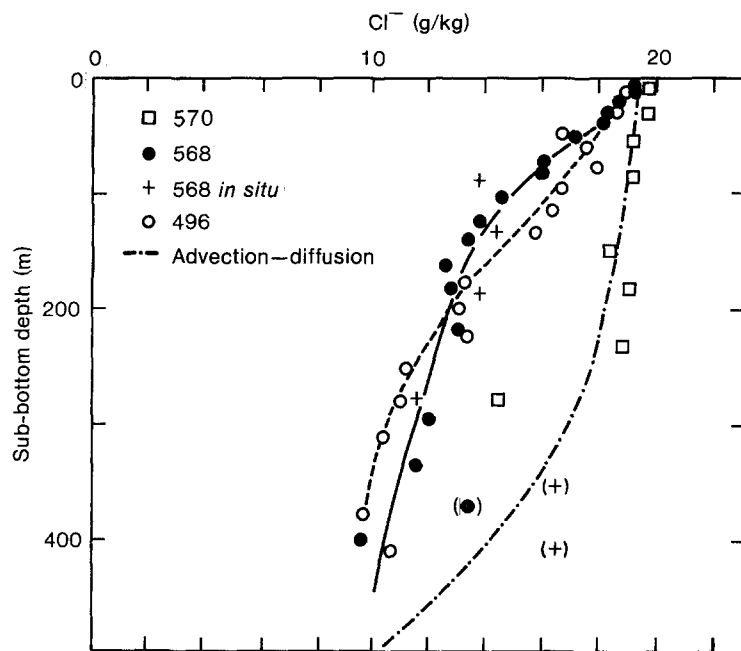


Fig. 7. Chlorinity-depth trends for DSDP sites 496, 568, and 570 (from [31] as modified by Finley and Krason (1986) [10]). Note that site 570 samples follow a diffusion profile (downward diffusion of chloride) in the upper part of the hole above 250 m subbottom depth where no hydrates were reported [31].

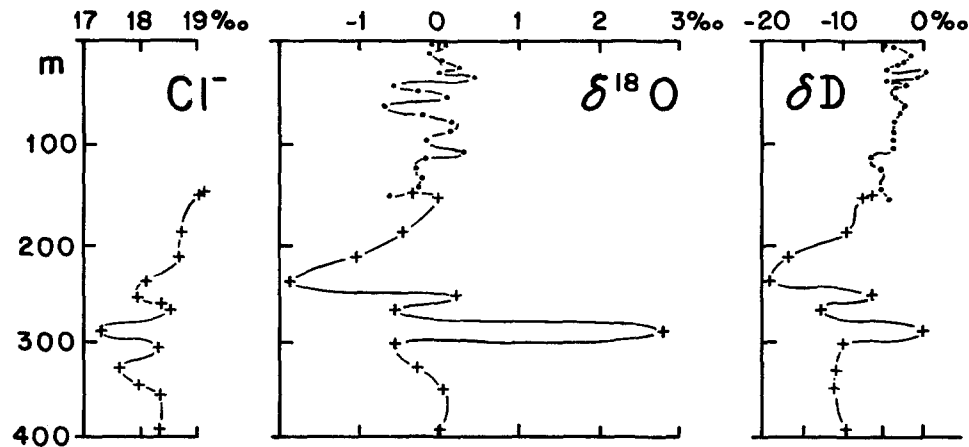


Fig. 8. Oxygen and hydrogen isotopic composition of squeezed pore waters from holes 533 (filled circles) and 533A (crosses), DSDP Leg 76 (from [46] Figure 4). Note that strongly positive hydrate-related $\delta^{18}\text{O}$ and δD anomalies near 290 m subbottom are preceded and followed by a decrease in δ -values. For explanation see Figure 9.

of the Leg 84 sites are attributed to substantially irregular concentrations of hydrates. So far, hydrates have been observed visually only in coarse-grained sediments such as ash layers (DSDP hole 498A [30]) or in massive gas-hydrate layers (DSDP hole 570 [45]), but not in fine-grained sediments. Jenden and Gieskes (1983) proposed a diffusion model to explain the particular shape of the hydrate-related spikes of the chlorinity and oxygen isotope anomalies [46] which underlines the importance of diffusion in removing excess chloride and partially replenishing the ^{18}O -deficit from the water left over in the pores after hydrate formation. Depending on time available and subsidence rates before hydrate decomposition, diffusion may substantially modify the composition of the residual pore water (Figure 9).

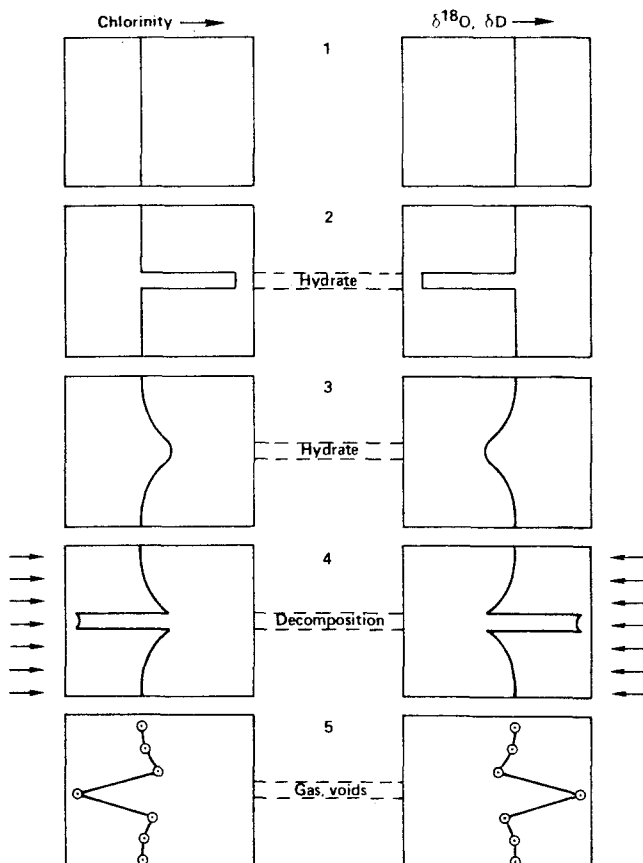


Fig. 9. Diffusion model to explain shape of chlorinity and $\delta^{18}\text{O}$ pore-water spikes associated with an isolated (decomposed) hydrate layer (from [46], Figure 5). 1: Chlorinity and $\delta^{18}\text{O}$, δD profiles before hydrate crystallization. 2: Hydrate crystallization withdraws fresh and isotopically heavy water and therefore raises chlorinity and lowers δ -values in the remaining pore-water. 3: Smoothed out concentration gradients by diffusion. 4: Hydrate decomposition in the sampled sediment superposes low-chlorinity and high δ -spikes on the partially decayed original anomalies. 5: Combined effects of 1 to 4, as measured after hydrate decomposition.

4. Discussion

Regarding the hydrate-decomposition mechanism for the pore-water anomalies in hydrate zones [9] the following problems warrant further discussion:

First, as outlined, the salt excluded from the hydrate structure should cause an increase in chlorinity in the pore water. It should be associated with a negative $\delta^{18}\text{O}$ anomaly. This effect should only be visible, however, at the top of the hydrate zone and in the sediments above, because due to the sampling artifact deeper within the hydrate zone it would be diluted. The chlorinity increase at the top is difficult to detect, first because hydrate formation often starts close to the sediment-water interface (sometimes within a meter or so below the sea floor), and rarely are sediments sampled that shallow in deep-sea drilling. The expected chlorinity increase above the hydrate zone may therefore have been overlooked in a number of deep-sea drill sites.

Secondly, a slight chlorinity increase may also result from the burial of saltier sea water during glacial epochs [47]. This effect, however, could be differentiated isotopically from the hydrate effect, because it would be associated with a positive $\delta^{18}\text{O}$ anomaly whereas the hydrate effect should cause a negative $\delta^{18}\text{O}$ anomaly (the opposite of the hydrate sampling artifact!).

Thirdly, the expected effect should be small for a hydrate zone extending upwards close to the sea floor because of the small corresponding chloride and $\delta^{18}\text{O}$ anomalies observed as sampling artifacts at the top of shallow hydrate zones. Its amplitude would be further decreased by diffusion if sedimentation rates are not too high.

The data from site 496 on the Guatemalan trench slope show a slight chlorinity increase in the top sample over the chlorinity of sea water, but the oxygen isotope ratio remains nearly unchanged (Figure 4). Thus the pore water data are inconclusive. The possible glacial signal and the hydrate signal, which would reinforce one another in the case of chloride, may have cancelled one another in the case of the oxygen isotopes. The uppermost sample of site 496 at 6.0 m subbottom depth was taken below the sulfate reduction zone (as no detectable sulfate is left, Figure 4) and from within the methane generation zone and probably also from within, rather than above the hydrate zone. Thus, hydrate decomposition may have released water and complicated the pore-water composition beyond recognition.

In site 497, the first sample at 4.5 m subbottom depth was obtained still from within the sulfate reduction zone and therefore most likely from above the top of the hydrate zone. Here, too, a small chlorinity increase over the chlorinity of sea-water is observed. The oxygen isotopes, however, show a slight positive anomaly, where a negative anomaly would be expected from upward diffusion of isotopically light water from the top of the hydrate zone which was probably located above the second sample at 16.0 m subsurface. Following the lines of reasoning above and taking high sedimentation rates into consideration (150 mm/ 10^3a for the Pleistocene of site 497 [48]), the chloride increase in the top sample at site 497 probably reflects a glaciation signal rather than a hydrate signal. Similar lines of reasoning apply to nearby site 568 of DSDP Leg 84 (Figure 4). Slight chlorinity increases in the top samples of sites 682, 685, and 688 of ODP Leg 112 have been interpreted as a hydrate-zone roof-effect [8] but this interpretation awaits confirmation by oxygen-isotopic analyses.

The more pronounced increase in salinity in the top part of hole 496 is not primarily hydrate-related, but due to other reactions which cause an increase e.g. in alkalinity and Mg. For this reason, in the foregoing discussion, chlorinity only has been considered rather than salinity because chlorinity is not affected by other diagenetic reactions at shallow burial levels.

Another problem closely related to the first one concerns efforts to obtain samples of pore waters under *in-situ* conditions from within the hydrate zone. Theoretically, such samples should not have been affected by the sampling artifact and would be expected to show increased chlorinities and lighter isotopes than the samples squeezed on board ship after hydrate decomposition.

Attempts during Leg 84 of the DSDP to obtain *in-situ* water samples with a pore-water sampler met only with limited success [31]. Of the six *in-situ* water samples obtained at site 568, at least two are diluted by sea water as can be seen e.g. from the increased sulfate content in sample # 5 (Figure 4). For sample # 6, no sulfate determination is available, but the elevated Mg content also suggests sea-water contamination.

Of the four samples considered reliable, two show minor (# 2, 3) increases in chlorinity, and two (# 1, 4) minor decreases compared to the samples squeezed on board; the same holds for salinity (Figure 4). Considering the small number of samples available and the small effects observed, results are inconclusive at present and clearly demonstrate the need for further *in-situ* sampling during drilling of hydrate zones in future ODP legs.

Encouraging for future *in-situ* sampling are the results of the few isotopic analyses available for the *in-situ* measurements of Leg 84. Both the oxygen and hydrogen isotopes for the *in-situ* samples considered reliable show a clear depletion in the heavy isotopes compared to the shipboard samples, as predicted by the hydrate-decomposition hypothesis (Figure 10). If these results can be reproduced and the chloride behaviour be resolved with new *in-situ* sample material in the future, the assumption of Hesse *et al.* (1985) [31] that hydrate decomposition had also affected the *in-situ* sampling process would have to be re-evaluated.

A third problem concerns site 565 (leg 84) on the Middle America trench slope off Costa Rica where more or less continuously downward decreasing chlorinity is associated with a $\delta^{18}\text{O}$ minimum between 95 and 170 m subbottom in the middle of the section penetrated (Figure 4).

There are two possibilities to explain this discrepancy. The first is that the decrease in chlorinity is caused by hydrate decomposition whereas the $\delta^{18}\text{O}$ minimum at mid-depth is the result of superposition of another isotope-fractionating process, namely alteration of volcanic glass to zeolites or smectites. If the two processes occur together, the effects of one cannot be separated from those of the other. Volcanic glass alteration can leave an imprint on pore-water $\delta^{18}\text{O}$ values as shown, for example by site 149 of the DSDP in the Caribbean Sea, where the minimum pore-water value caused by this mechanism is $-2\text{\textperthousand}$ [25]. The $\delta^{18}\text{O}$ minimum for site 565 is $-1.26\text{\textperthousand}$. Volcanic glass in site 565 is abundant above core 12 (120 m subbottom depth), where up to 20% and more have been recorded in smear slides. Below that depth, that is, the depth where the $\delta^{18}\text{O}$ decrease occurs, volcanic glass is very sparse (Figure 11). Only traces of 1 to 2% have been reported [49]. This might indicate diagenetic alteration and disappearance of glass which was

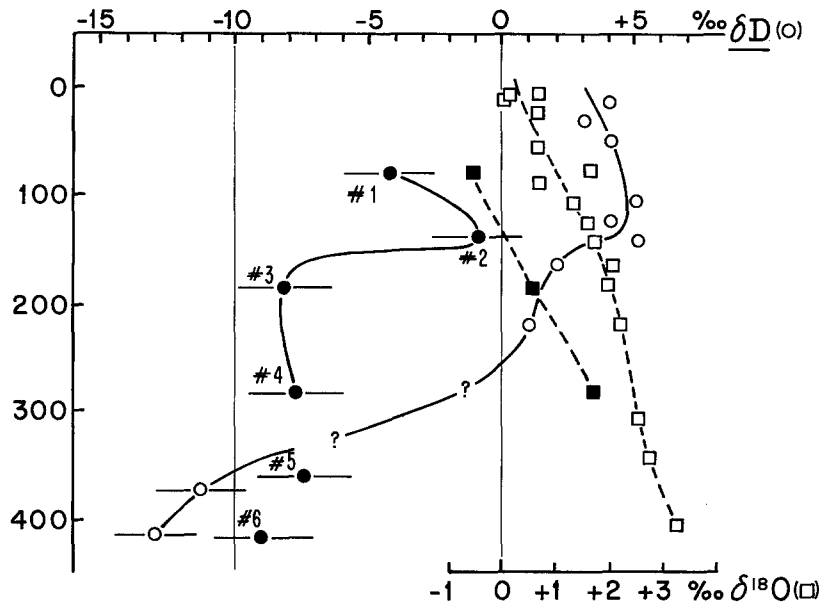


Fig. 10. Comparison of *in-situ* (filled symbols) and shipboard (open symbols) δD (circles) and $\delta^{18}\text{O}$ (squares) measurements for site 568, DSDP Leg 84. *In-situ* water samples #5 and #6 for δD are considered unreliable because of sea-water contamination. δD values of *in-situ* samples and the lowermost two samples squeezed onboard – courtesy P. D. Jenden; remaining hydrogen isotopic analyses – courtesy J. R. Lawrence.

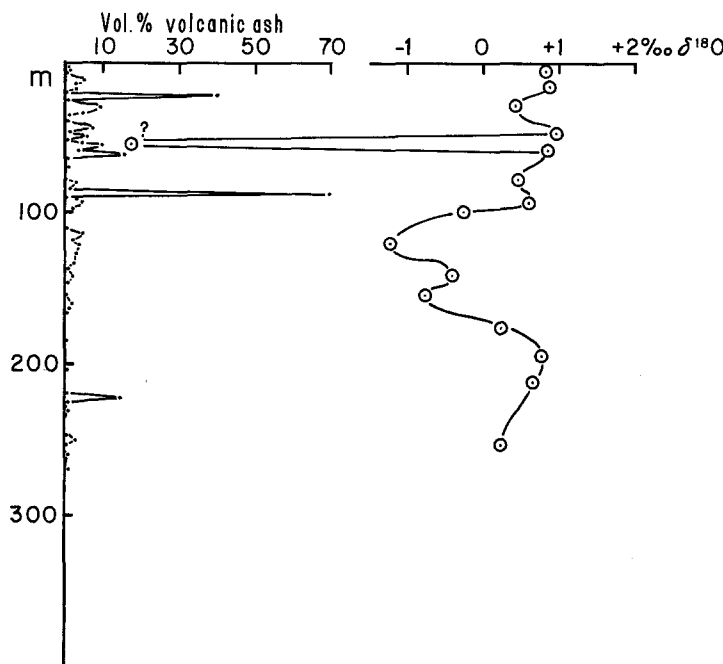


Fig. 11. Distribution of volcanic glass in smear slides (from [49]) and $\delta^{18}\text{O}$ interstitial-water results (from [31]) for site 565, Middle America trench slope off Costa Rica. See text for explanation.

formerly present and would explain the negative oxygen isotope anomaly. Finley and Krason [10, p. 138] argue that other drill-sites of DSDP legs 67 and 84 which contain more volcanic ash than site 565 should therefore also show a negative $\delta^{18}\text{O}$ anomaly rather than the positive anomalies that were observed [10]. In these instances, high concentrations of volcanic glass, however, were reported down to the bottom of the holes indicating that glass *alteration* may not have taken place to the same extent as at site 565.

The second possibility is that hydrates are absent from the depth interval in question. This would be in accordance with the shipboard observation for this site that high gas concentrations occur only below 175 m. The chlorinity decrease might then be due to meteoric water influx which would be a significant finding, because of the great water depth where it occurs (3111 m for site 565). Considerable advective flow rates would be required to prevent this water from becoming salty during its passage through a several km thick sediment column and along horizontal migration distances of several tens of km.

A fourth problem is the magnitude of the isotopic fractionation attributed to hydrate formation and the nonlinear correlation between this effect and the associated salt-fractionation effect shown by the curvature of the lines plotted in Figure 12. The heaviest waters (in terms of their oxygen isotopes) encountered at the bottom of sites 496 ($\delta^{18}\text{O} = 2.59\text{\textperthousand}$ at 380.5 m subbottom), and 568

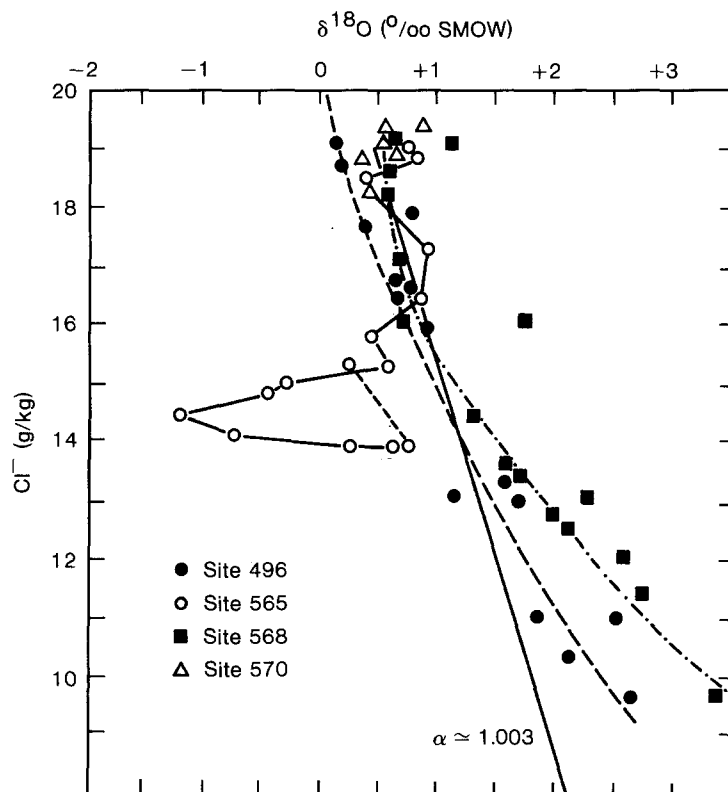


Fig. 12. Nonlinear chlorinity-oxygen isotope correlations (from [31] Fig. 5).

($\delta^{18}\text{O} = 3.31\text{\textperthousand}$ at 401.7 m subbottom), respectively are too heavy to be obtained by a single-step fractionation. As pointed out by Hesse *et al.* [31], if 50% of the pore-water at the bottom of the hydrate zone had crystallized as gas hydrate, the isotope fractionation associated with this volume should lead to a maximum ^{18}O enrichment of $\delta = 1.35\text{\textperthousand}$ [31]. With a water-hydrate fractionation factor of 1.027 for oxygen [50], even complete solidification of the pore water would not yield $\delta^{18}\text{O}$ values higher than $2.7\text{\textperthousand}$, but in this case the pore water taken from the sediment after hydrate decomposition should be fresh-water, rather than saline water with about 8 or $9.5\text{\textperthousand}$ chlorinity. Although the observed high $\delta^{18}\text{O}$ values can be obtained by multiple fractionation at the base of the hydrate zone [31] this mechanism should produce much lower chlorinities than observed. This discrepancy between chloride content and $\delta^{18}\text{O}$ values might be caused by chloride ions trapped between rapidly formed hydrate crystals. This idea will not be easy to test, but would yield the observed nonlinear trend in the Cl^- versus $\delta^{18}\text{O}$ curves.

5. Conclusions

As the foregoing discussion has shown, details of the relationship between pore-water anomalies and the occurrence of gas-hydrates in deep-sea sediments of the continental slopes and rises are far from having all been resolved and clearly demonstrate the need for further careful studies. Existing problems should, however, not distract from the fact that the hydrate decomposition mechanism as a whole has been successful in explaining hydrate-related pore-water anomalies. Ways for solving open problems have been pointed out in this paper. Future detailed research through carefully integrated studies on samples obtained from deep ocean drilling should provide a solution to the problems that still exist.

Acknowledgements

The author's research on diagenesis has been supported by the Natural Sciences and Engineering Research Council of Canada, grant no. OGP 0007368. The author wishes to thank P. D. Jenden and J. R. Lawrence who provided the hydrogen isotopic analyses for Figure 10.

References

1. S. L. Miller: 'The nature and occurrence of clathrate hydrates'. *Natural Gases in Marine Sediments*, Marine Sci. v.3, Ed. I. R. Kaplan, 1974, pp. 151–177.
2. W. A. Sokolov: *Geochemistry of Gases of the Earth's Atmosphere*, 301 pp., Nedra, Moscow, 1966 (in Russian).
3. R. D. Stoll, J. Ewing, and G. B. Bryan: *J. Geophys. Res.* **76**, 2090 (1971).
4. T. H. Shipley, and B. M. Didyk: 'The occurrence of methane hydrates offshore southern Mexico'. (Init. Repts. Deep Sea Drilling Proj. vol. 66), pp. 547–555. U.S. Govt. Print. Off. 1982.
5. W. E. Harrison and J. A. Curiale: 'Gas hydrates in sediments of holes 497 and 498 A, Deep Sea Drilling Project Leg 67'. Init. Repts. Deep Sea Drilling Proj. vol. 67, J. Aubouin, R. von Huene, *et al.*, pp. 591–594. U.S. Govt. Printing Office 1982.
6. A. G. Yefremova and B. P. Zhizhchenko: *Doklady Earth Sci. Sect.* **214**, 1179 (1974).

7. K. A. Kvenvolden and L. A. Barnard: 'Gas hydrates of the Blake Outer Ridge, Site 533, DSDP Leg 76.' Init. Repts. Deep Sea Drilling Proj. vol. 76, R. E. Sheridan, F. M. Gradstein, *et al.* U.S. Govt. Print. Off. 1983, pp. 353-366.
8. K. A. Kvenvolden and M. Kastner 'Gas hydrates of the Peruvian continental margin' Proc., Ocean Drilling Progr. vol. 112, E. Suess, R. von Huene, *et al.* (in press).
9. R. Hesse and W. E. Harrison: *Earth Planet. Sci. Lett.* **55**, 453 (1981).
10. P. Finley and J. Krason: 'Formation and stability of gas hydrates of the Middle America Trench'. Geological evolution and analysis of confirmed or suspected gas hydrate localities, vol. 9, Geo-explorers International, 243 pp., U.S. Dept. of Energy, Morgantown, WV 1986.
11. P. D. Finley and K. L. Dominic: *Am. Chem. Soc. Div. Geochem.*, Abstr. no. 3 1988.
12. F. T. Manheim and F. L. Sayles: 'Composition and origin of interstitial waters of marine sediments, based on deep sea drill cores'. *Marine Chemistry, The Sea* vol. 5, Ed. E. D. Goldberg, Wiley 1974, pp. 527-568.
13. F. L. Sayles and F. T. Manheim: *Geochim. Cosmochim. Acta* **39**, 103 (1975).
14. J. M. Gieskes: *Ann. Rev. Earth Planet. Sci.* **3**, 433 (1975).
15. J. M. Gieskes: 'Deep Sea drilling interstitial-water studies: Implications for chemical alteration of the ocean crust, Layers I and II'. *The Deep Sea Drilling Project: A Decade of Progress*, Soc. Econ. Paleontologists Mineralogists Spec. Publ. v.32, Ed. J. E Warme, R. J. Douglas, and E. L. Winterer, 1981.
16. J. M. Gieskes: 'The chemistry of interstitial waters of deep-sea sediments: Interpretation of Deep Sea Drilling Data'. *Chem. Oceanogr.* vol. 8, Ed. J. P. Riley and R. Chester, 1983, pp. 221-269.
17. R. E. McDuff: *Geochim. Cosmochim. Acta* **45**, 1705 (1981).
18. R. Hesse: Diagenesis. (Geol. Assoc. Canada, Reprint Ser. v. 4. Ed. I. A. McIlreath) (in press).
19. R. N. Anderson, M. G. Langseth, and J. G. Sclater: *J. Geophys. Res.* **82**, 3391 (1977).
20. R. N. Anderson, M. A. Hobart, and M. G. Langseth: *Science* **204**, 828 (1979).
21. U. Fehn: *Econ. Geol.* **81**, 1396 (1986).
22. R. D. Hyndman, M. G. Langseth, and R. P. Von Herzen: 'A review of Deep Sea Drilling Project geothermal measurements through Leg 71'. Init. Repts. Deep Sea Drilling Proj. vol. 78B, R. D. Hyndman, M. H. Salisbury, *et al.* U.S. Govt. Print. Off. 1985, pp. 813-823.
23. R. E. McDuff and J. M. Gieskes: *Earth Planet. Sci. Lett.* **33**, (1976).
24. R. E. McDuff: 'Conservative behavior of calcium and magnesium in interstitial waters of marine sediments: Identification and interpretation. Unpubl. Ph.D. thesis, Scripps Institution of Oceanography, 183 pp., 1978.
25. J. R. Lawrence, J. M. Gieskes, and W. S. Broecker: *Earth Planet. Sci. Lett.* **27**, 1 (1975).
26. J. M. Gieskes and J. R. Lawrence: *Geochim. Cosmochim. Acta* **45**, 1687 (1981).
27. P. N. Froelich, G. P. Klinkhammer, M. L. Bender, N. A. Luedtke, G. R. Heath, D. Cullen, P. Dauphin, D. Hammond, B. Hartman, and V. Maynard: *Geochim. Cosmochim. Acta* **43**, 1075 (1979).
28. G. E. Claypool and I. R. Kaplan: 'The origin and distribution of methane in marine sediments'. *Natural Gases in Marine Sediments*. Marine Sci. vol. 3, Ed. I. R. Kaplan, Plenum Press, 1974 pp. 99-140.
29. G. E. Claypool, C. N. Threlkeld, P. N. Mankiewicz, M. Arthur, A. and T. F. Anderson: 'Isotopic composition of interstitial fluids and origin of methane in slope sediment of the Middle America Trench, Deep Sea Drilling Project Leg 84'. Init. Repts. Deep Sea Drilling Proj. vol. 84, R. Von Huene, J. Aubouin, *et al.* U.S. Govt. Print. Off. 1985, pp. 683-691.
30. W. E. Harrison, R. Hesse, and J. M. Gieskes: 'Relationship between sedimentary facies and interstitial water chemistry in slope, trench, and Cocos plate sites from the Mid-America Trench transect, active margin off Guatemala. Leg 67, DSDP'. Init. Repts. Deep Sea Drilling Proj. vol. 67, J. Aubouin, R. von Huene, *et al.* U.S. Govt. Print. Off. 1982, pp. 603-614.
31. R. Hesse, J. Lebel, and J. M. Gieskes: 'Interstitial water chemistry of gas hydrate bearing sections on the Middle America trench slope, Deep Sea Drilling Project, Leg 84'. Init. Repts. Deep Sea Drilling Project, vol. 84, R. von Huene, J. Aubouin, *et al.* U.S. Govt. Print. Off. 1985, pp. 727-737.
32. P. J. Mueller: *Geochim. Cosmochim. Acta* **41**, 765 (1977).
33. ODP Leg 110 Scientific Party: *Nature* **326**, 785.
34. J. M. Brooks, M. C. Kennicutt, R. R. Fay, T. J. McDonald, and R. Sassen: *Science* **225**, 409 (1984).
35. J. M. Brooks, H. B. Cox, W. R. Bryant, M. C. Kennicutt II, R. G. Mann, and T. J. McDonald: *Adv. Organ. Geochem.* **10**, 221 (1986).

36. J. M. Brooks, M. C. Kennicutt II, R. Bidigare, T. L. Wade, E. N. Powell, G. L. Denoux, R. R. Fay, J. J. Childress, C. R. Fisher, I. Rossman, and G. Boland: *Eos* **68**, 498 (1987).
37. J. M. Brooks, M. C. Kennicutt II, and R. C. Pfleiderer: *Am. Chem. Soc. Div. Geochem. Abstr.*, no. 4 (1988).
38. M. E. Field and K. A. Kvenvolden: *Geology* **14**, 537 (1986).
39. M. Schoell: *Am. Assoc. Petroleum Geologists Bull.* **67**, 2225 (1983).
40. P. D. Jenden and I. R. Kaplan: *Appl. Geochem.* **1**, 631 (1986).
41. R. K. Schecki, and L. S. Land: *Geochim. Cosmochim. Acta* **47**, 1487 (1983).
42. Land, personal communication (1987).
43. J. Azema, J. Bourgois, P. O. Baumgartner, J. Tournon, A. Desmet, and J. Aubouin: 'A tectonic cross-section of the Costa Rican Pacific littoral as a key to the structure of the landward slope of the Middle America trench off Guatamala'. Init. Repts. Deep Drilling Proj. vol 84, R. von Huene and J. Aubouin, *et al.* U.S. Govt. Print. Off. Washington, D.C. 1985, pp. 831-850.
44. J. M. Gieskes, K. Johnston, and M. Boehm: 'Interstitial water studies, Leg 66'. Init. Repts. Deep Sea Drilling Proj. vol. 84, R. von Huene, J. Aubouin, *et al.* U.S. Govt. Print. Off., Washington, D.C. 1985, pp. 961-967.
45. K. A. Kvenvolden and T. J. McDonald: 'Gas hydrates of the Middle America Trench'. Init. Repts. Deep Sea Drilling Proj. vol. 84, R. von Huene and J. Aubouin *et al.* U.S. Govt. Print. Off. Washington, D.C. 1985, pp. 667-682.
46. P. D. Jenden and J. M. Gieskes: 'Chemical and isotopic composition of interstitial water from Deep Sea Drilling Project sites 533 and 534'. Init. Repts. Deep Sea Drilling Proj. vol. 76, R. E. Sheridan, and F. M. Gradstein *et al.* U.S. Govt. Print. Off., Washington, D.C. 1983, pp. 453-461.
47. R. E McDuff: 'The chemistry of interstitial waters, Deep Sea Drilling Project Leg 86'. Init. Repts. Deep Sea Drilling Proj. vol. 86, G. R. Heath and L. H. Burckle *et al.* U.S. Govt. Print. Off., Washington, D. C. 1985, pp. 675-687.
48. R. von Huene, J. Aubouin, J. Azema, G. Blackinton, J. A. Carter, W. T. Coulbourn, D. S. Cowan, J. A. Curiale, C. A. Dengo, R. W. Faas, W. Harrison, R. Hesse, D. M. Hussong, J. W. Ladd, N. Muzylov, T. Shiki, P. R. Thompson, and J. Westberg: *Geol. Soc. Am. Bull.* **91**, 421 (1980).
49. 'DSDP Leg 84, Shipboard Scientific Party: Site 565'. Init. Repts. Deep Sea Drilling Proj., vol. 84, R. von Huene and J. Aubouin *et al.* U.S. Govt. Print. Off. 1985, pp. 21-77.
50. D. W. Davidson, D. G. Leaist, and R. Hesse: *Geochim. Cosmochim. Acta* **47**, 2293 (1983).